

Hall and ion-slip current efficacy on thermal performance of magnetic power-law hybrid nanofluid using modified Fourier's law

N. Sultana^a, S. Shaw^b, S. Mondal^c, M.K. Nayak^d, S. Nazari^{e,*}, Abir Mouldi^f, Ali J. Chamkha^g

^a Department of Mathematics, Amity University, Kolkata 700135, West Bengal, India

^b Department of Mathematics and Statistical Sciences, Botswana International University of Science and Technology, Private Bag 16, Palapye, Botswana

^c Department of Mathematics, North-Eastern Hill University, Shillong-793022, Meghalaya, West Bengal, India

^d Department of Mechanical Engineering, ITER, Siksha 'O' Anusandhan Deemed to be University, Bhubaneswar 751030, India

^e Young Researchers and Elite Club, Islamic Azad University, Tehran, Iran

^f Department of Industrial Engineering, College of Engineering, King Khalid University, Abha 61421, Saudi Arabia

^g Faculty of Engineering, Kuwait College of Science and Technology, Doha District, Kuwait

ARTICLE INFO

Keywords:

Power-law model
Magnetic HNF
Hall effect
Modified Fourier's law
Stretching sheet

ABSTRACT

Magnetohydrodynamic free convection liquid considering Hall along with ion-slip current has many engineering usages. In addition, boundary layer flow of power-law fluids due to a stretching plane possesses sundry applications in biological sciences, geophysics, and petroleum industries. Further, hybrid nanofluids are important due to their high heat transfer capability. In view of such relevance, the goal of this investigation is to analyze Hall along with ion-slip effects on thermo-fluidic flow of magnetic power-law hybrid nanofluid so as to accomplish effective cooling in the desired thermal systems. Present investigation's novelty is adding hybrid nanostructure to power-law fluid flow influenced by Hall and ion-slip mechanism and implementation of modified Fourier's law featured with velocity and temperature gradients. The key results are that fluid velocity amplifies with rise in ion-slip and Hall parameters. Modified Prandtl numbers and Hall parameter ameliorate heat transfer rate while ion-slip parameter diminishes it.

1. Introduction

Many researchers have been inspired over the years to study flow and heat transfer (HT) over an extendable surface because of its numerous important engineering utilizations, like rapid spray cooling, glass blowing, polymer extrusion, and microelectronics' cooling. The primary pioneer to examine the boundary layer flow (BLF) on stretched surfaces theoretically was Crane [1]. Since then, many scholars [2–9] have come forward to contribute to our understanding of many facets of flow and HT issues embodying stretched planes. Further, the influence of interior heat production/absorption (Mukhopadhyay and Vajravelu [10]), mass transfer (Mukhopadhyay et al. [11]), thermal stratification (Mukhopadhyay et al. [12]), partial slip (Mukhopadhyay et al. [13]), and chemical reaction (Mukhopadhyay [14]) subject to the flow of disparate fluids over sundry stretched surfaces have been studied well.

Nomenclature

(u, v, w) velocity along (x, y, z) directions
HT heat transfer

(continued)

| | |
|---|---|
| HNF | hybrid nanofluid |
| MHD | magnetohydrodynamic |
| PLF | power-law fluid |
| PLHNF | power-law hybrid nanofluid |
| ODE | ordinary differential equation |
| PDE | partial differential equation |
| $\rho_{hnf}, \rho_{nf}, \rho_f, \rho_{s_1}, \rho_{s_2}$ | effective density of HNF, nanofluid, base fluid, Cu, TiO ₂ (kg m ⁻³) |
| $(\rho C_p)_{hnf}, (\rho C_p)_{nf}, (\rho C_p)_f, (\rho C_p)_{s_1}, (\rho C_p)_{s_2}$ | specific heat capacity of the HNF, nanofluid, base fluid, Cu, TiO ₂ |
| $\mu_{hnf}, \mu_{nf}, \mu_f$ | effective dynamic viscosity of HNF, nanofluid, base fluid |
| $k_{hnf}, k_{nf}, k_f, k_{s_1}, k_{s_2}$ | thermal conductivity of HNF, nanofluid, base fluid, Cu, TiO ₂ |
| $\sigma_{hnf}, \sigma_f, \sigma_{s_1}, \sigma_{s_2}$ | electrical conductivity of HNF, nanofluid, base fluid, Cu, TiO ₂ |
| $\beta_{hnf}, \beta_f, \beta_{s_1}, \beta_{s_2}$ | thermal expansion coefficient of HNF, base fluid, Cu, TiO ₂ |
| $\nu_{hnf}, \nu_{nf}, \nu_f$ | kinematic viscosity of HNF, nanofluid, base fluid |

(continued on next page)

(continued on next column)

* Corresponding author.

E-mail address: son.nazari@gmail.com (S. Nazari).

<https://doi.org/10.1016/j.asej.2024.102838>

Received 17 December 2023; Received in revised form 20 February 2024; Accepted 26 April 2024

Available online 4 May 2024

2090-4479/© 2024 THE AUTHORS. Published by Elsevier BV on behalf of Faculty of Engineering, Ain Shams University. This is an open access article under the CC BY-NC-ND license (<http://creativecommons.org/licenses/by-nc-nd/4.0/>).

(continued)

| | |
|----------------------|---|
| λ | stretching ratio |
| ϕ_1, ϕ_2 | solid volume fractions for Cu and TiO ₂ respectively |
| T | fluid temperature |
| T_∞ | ambient fluid temperature |
| T_w | temperature at the surface of the sheet |
| T_{ref} | reference temperature |
| u_w | stretching velocity |
| τ_{ij} | Cauchy stress tensor |
| n | power-law index |
| Γ_1, Γ_2 | positive constants |
| Υ | flow consistency index |
| q | heat flux |
| Ω | angular velocity |
| β_e | ion-slip parameter |
| β_i | Hall parameter |
| h_f | heat transfer coefficient |
| $a (> 0)$ | stretching constant |
| M | magnetic parameter |
| K | buoyancy parameter |
| Pr_1 | first modified Prandtl number |
| Pr_2 | second modified Prandtl number |
| Pr_3 | third modified Prandtl number |
| Bi_1 | first modified Biot number |
| Bi_2 | second modified Biot number |
| Bi_3 | third modified Biot number |
| hnf: | hybrid nanofluid |
| f: | base fluid |
| s_1 | first nanoparticle (Cu) |
| s_2 | second nanoparticle (TiO ₂) |

Industrial and regular liquids do not comply with the Newton's law of viscosity as the viscosity of said fluids is not consistent with the strain rate. This type of fluids is known as non-Newtonian fluid. Among these fluids, there are some non-Newtonian liquids that exhibit properties where the rate of shear is not independent of the direction of the flow [15–19]. These shear-rate dependent fluids can further be classified into different classes such as Casson fluids, Herschel–Bulkley, Carreau–Yasuda fluids, Bingham fluids, Power-Law fluids and Carreau fluids. Among these, Power-Law fluids have garnered much attention of scholars due to their various technological and industrial usages, like hydrocarbon oils, drilling mud, chemical catalytic reactors or heat exchangers, paints, greases, geothermal energy systems etc [20–22].

In the past ten years, a growing number of researchers have become interested in studying nanofluids due to their intriguing and important engineering focus. These applications and uses embody safer surgery, cooling in cancer therapy, transportation, solid state lighting, extremely powerful computers, military-grade electronic devices, biomedicine, and various process industries etc. The primary goal of using nanofluids in these kinds of systems is to improve heat transfer capacity and thermal conductivity in order to get superior cooling. Choi discovered this through experimentation [23]. Further progress in the relevant study was made by Xie et al. [25] and Eastman et al. [24], who demonstrated that the use of nanofluids may achieve greater thermal conductivities in thermal systems. Moreover, Ghosh and Mukhopadhyay [26] investigated the HT and flow of NF over a porous sheet that is exponentially diminishing. They discovered that when the Lewis number rises, the heat transmission rate may decrease. A computational study of NF over an upright wedge was conducted by Abbas et al. [27]. It was discovered that increasing the velocity slip parameter increased the rate of HT. Increasing the amount of solid nanoparticles decreased the thickness of the momentum BL. Additionally, a mathematical model of the temperature-dependent power-law NF flow over a changeable expandable Riga plane was created by Abbas et al. [28]. They found that temperature profiles significantly increased with increase in Eckert number, thermophoresis and heat production parameters, but not with the Prandtl number. Moreover, the related works such as Jeffrey NF flow over an oscillatory stretchable surface (Awan et al. [29]), micropolar NF over a nonlinear stretched Riga surface (Abbas et al. [30]), and Newtonian/.non-Newtonian nanofluid flow over deformed surfaces

(Nayak et al. [31–34]) were conducted effectively.

To further increase the heat transferring abilities of nanofluids, researchers came up with the ideas of hybrid nanofluids (HNFs) as extension of nanofluids in more recent years. These fluids are believed to have improved thermophysical and rheological properties and better heat transferring ability. HNFs are obtained by incorporating more than one kind of nanomaterials in the base fluid. Many research papers so far have suggested significant improvement in heat transfer (HT) in heat exchangers due to the usage of HNFs and also the potential of more improvement with the help of further research on topics such as the different combinations of the nanoparticles, the mixing ratio etc. The applications of HNFs include industrial cooling agents, smart fluids, cancer treatment, liquid cooling of processors etc. Sultana et al. [35] studied flow with hybrid nanostructure. Babu et al. [36] examined some results tied to how hybrid nano-composites helped HT in base fluids and also some applications related to it. Cimpean et al. [37] studied the convective HT of HNF in a porous medium. Sadiq [38] has included the fundamental law of heat transport in fluid to the power-law rheological model with thermophysical features. In light of these facts, Zeeshan et al. [39] used the Modified Fourier Law to analyse the melting heat effect on ethylene–glycol based nanofluid and HNF through a curved surface. The related works were observed in [40–44]. The energy and mass transmission of a power-law liquid was studied by Cheng [45]. Flow of a power-law fluid (PLF) over a stretchable surface under suction/ injection, thermal radiation, and magnetohydrodynamic (MHD) conditions was studied by Mahapatra et al. [46]. The works dealing with the impact of MHD subject to non-Newtonian fluid flow are visualized in [47–49].

When a liquid is partially ionized, it displays distinct properties from regular liquids under the efficacy of MHD and in this case the partially ionized fluid faces the Hall force as the consequences of ion force, magnetic force and electrons' collision. One of the processes to generate these Hall currents in a partially ionized stream is to incorporate Ohm's law [50] together with the laws from Maxwell's equation. Nawaz et al. [51] perused the MHD flow of partially ionized liquids following the aforementioned laws. Free stream velocity as well as Hall currents' impacts on a movable plane under a magnetic field were examined by Takhar et al. [52]. Krishna et al. [53] researched the impacts of Hall as well as ion-slip on rotating magnetized flow that is unsteady and free convective. Utilizing the Casson theory, Nazir and Mukdasai [54] explored impact of viscous dissipation and Hall effects on the movement of ethylene glycol carrying titania, silica and alumina nanomaterials. Elsaid and AlShurafat [55] explored the efficacy of Joule heating and Hall current on a spinning hybrid radiative NF over a stretchable plane.

From the literature survey, it is revealed that many researchers have worked on the flow and thermal analysis of PLFs, nanofluids over several stretched surfaces subject to different boundary conditions of motion. However, the flow and thermal analysis of power-law HNF over a stretched sheet subject to modified Fourier's law featured with temperature and velocity gradients is yet to be published. In view of the relevance of power-law fluids/nanofluids and superior thermophysical properties of HNFs, and in order to bridge the gap in the existing literature, authors have been motivated to carry out the investigation in the related aspects.

The objective of the present investigation would be to analyze the flow and thermal analysis of power-law HNF over a stretched sheet subject to modified Fourier's law with temperature and velocity gradients. The novelties would be as follows:

- Introduction of Fourier's law modified by temperature and velocity gradients.
- Consideration of the Hall along with ion-slip effects on the power-law fluid with hybrid nanostructure (Cu + TiO₂ + EG).

The current study may contribute the very effective cooling to the industrial thermal systems embodying HNFs flow subject to Hall along

with ion-slip mechanism.

2. Formulation of the problem

We consider magneto-power-law fluid flow with hybrid nanostructure ($Cu + TiO_2 + EG$) past stretched linear sheet subject to Hall current and Joulean dissipation. The HNF comprises of ethylene glycol (EG) as base fluid and Cu & TiO_2 as nanoparticles. The stretching velocity of linear sheet is assumed as $u_w = \lambda x$ (λ is stretching rate; s^{-1}). Assume that positive y-axis is parallel to plate's surface, positive z-axis is normal to plane xy, and positive x-axis is measured in the direction of fluid motion as portrayed in Fig. 1. An external magnetic field of uniform strength B_0 is imposed normal to the sheet. The values of HNF's thermo-physical features are mentioned in Table 1. The suppositions of the present study would be as follows:

- The flow may well be incompressible and steady.
- Hall effect and ion-slip mechanism are introduced.
- Joulean dissipation is assumed.
- The base fluid (ethylene glycol) and nanomaterials (Cu & TiO_2) would be in thermic equilibrium.
- Power-law fluid model is adopted.
- Modified Fourier's law is introduced.

The power-law Cauchy stress tensor is defined as (Bird [56])

$$\tau_{ij} = -Y \left| \sqrt{0.5(\Omega \bullet \Omega)} \right|^{-(1-n)} \Omega$$

here n, Y, Ω are respectively power-law index, flow consistency index, and symmetrical rate of deformation tensor. The above relation for $0 < n < 1$ specifies Pseudo-plastic stream, $n > 1$ describes dilatant liquid and $n = 1$ represents Newtonian fluid.

The PLF formulation in the form of shear stress along x and z directional components are expressed as (Bird [56])

$$\tau_{yx} = Y \left| \frac{\partial u}{\partial y} \right|^{n-1} \frac{\partial u}{\partial y}, \quad \tau_{zx} = Y \left| \frac{\partial w}{\partial y} \right|^{n-1} \frac{\partial w}{\partial y}$$

Based on thermal conductivity affected by both velocity gradient [57] and temperature gradient [58], a modified Fourier's law is introduced as

$$q = k_{hnf} \left(\Gamma_1 \left| \frac{\partial u}{\partial y} \right|^{n-1} + \Gamma_2 \left| \frac{\partial T}{\partial y} \right|^{n-1} \right) \frac{\partial T}{\partial y}$$

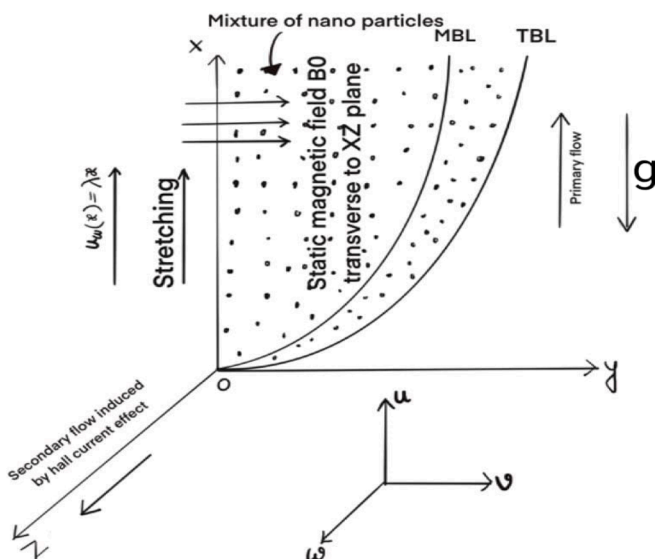


Fig. 1. Flow geometry.

Table 1

Nanofluid's thermo-physical features(Si et al. [34], Aziz et al. [35]).

| | $\rho(Kg/m^3)$ | $C_p(J/KgK)$ | $k(W/mK)$ | $\beta \times 10^{-5} \left(\frac{1}{K} \right)$ | $\sigma(Sm^{-1})$ |
|-----------------|----------------|--------------|-----------|---|----------------------|
| Ethylene Glycol | 1114 | 2415 | 0.252 | 57 | 5.5×10^{-6} |
| Cu | 8933 | 385 | 400 | 1.67 | 5.96×10^7 |
| TiO_2 | 4250 | 686.2 | 8.9538 | 0.9 | 2.38×10^6 |

where q displays the heat flux, T describes the temperature, k_{hnf} would be thermal conductivity, Γ_1 & Γ_2 are positive constants and represent different weights such that $\Gamma_1 + \Gamma_2 = 1$.

Based on the modified Fourier's law, the convective HT at the stretched surface is modified as

$$k_{hnf} \left(\Gamma_1 \left| \frac{\partial u}{\partial y} \right|^{n-1} + \Gamma_2 \left| \frac{\partial T}{\partial y} \right|^{n-1} \right) \frac{\partial T}{\partial y} = h_f (T - T_w)$$

Using above mentioned assumptions and Hall effect along with ion-slip concepts, governing equations are [2,18,51,53,57,58]:

$$u \frac{\partial u}{\partial x} + v \frac{\partial v}{\partial y} = 0 \tag{1}$$

$$u \frac{\partial u}{\partial x} + v \frac{\partial u}{\partial y} = \nu_{hnf} \frac{\partial}{\partial y} \left(\left| \frac{\partial u}{\partial y} \right|^{n-1} \frac{\partial u}{\partial y} \right) + \frac{g^* (\rho\beta)_{hnf} (T - T_\infty)}{\rho_{hnf}} - \frac{\sigma_{hnf} B_0^2 (1 + \beta_e \beta_i) u - \beta_e w}{\rho_{hnf} [\beta_e^2 + (1 + \beta_e \beta_i)^2]} \tag{2}$$

$$u \frac{\partial w}{\partial x} + v \frac{\partial w}{\partial y} = \nu_{hnf} \frac{\partial}{\partial y} \left(\left| \frac{\partial w}{\partial y} \right|^{n-1} \frac{\partial w}{\partial y} \right) + \frac{g^* (\rho\beta)_{hnf} (T - T_\infty)}{\rho_{hnf}} - \frac{\sigma_{hnf} B_0^2 [(1 + \beta_e \beta_i) w + \beta_e u]}{\rho_{hnf} [\beta_e^2 + (1 + \beta_e \beta_i)^2]} \tag{3}$$

$$u \frac{\partial T}{\partial x} + v \frac{\partial T}{\partial y} = \alpha_{hnf} \frac{\partial}{\partial y} \left\{ \left(\Gamma_1 \left| \frac{\partial u}{\partial y} \right|^{n-1} + \Gamma_2 \left| \frac{\partial w}{\partial y} \right|^{n-1} \right) \frac{\partial T}{\partial y} \right\} + \frac{\sigma_{hnf} B_0^2 (u^2 + w^2)}{(\rho c_p)_{hnf} [\beta_e^2 + (1 + \beta_e \beta_i)^2]} \tag{4}$$

With boundary conditions [59]:

$$\left. \begin{aligned} u = u_w = \lambda x, v = 0, w = 0, \\ k_{hnf} \left(\Gamma_1 \left| \frac{\partial u}{\partial y} \right|^{n-1} + \Gamma_2 \left| \frac{\partial w}{\partial y} \right|^{n-1} + \Gamma_3 \left| \frac{\partial T}{\partial y} \right|^{n-1} \right) \frac{\partial T}{\partial y} = h_f (T - T_w) \text{ at } y = 0 \\ u \rightarrow 0, w \rightarrow 0, T \rightarrow T_\infty \text{ as } y \rightarrow \infty \end{aligned} \right\} \tag{5}$$

Here, (u, v, w) are velocities, g^* would be gravitational constant, $\rho_{hnf}, \mu_{hnf}, \beta_{hnf}, \sigma_{hnf}, k_{hnf}, (\rho C_p)_{hnf}$ are density, dynamic viscosity, thermal expansion coefficient, electrical conductivity, thermal conductivity, specific heat capacity of HNF, Ω indicates angular velocity, n is power-law index, β_e & β_i are ion-slip and Hall parameters, T is temperature of HNF, T_∞ would be the ambient temperature, T_w is temperature at the plane's surface, and h_f is HT coefficient, $a > 0$ is stretching constant, $\Gamma_1, \Gamma_2, \Gamma_3$ are positive constants so that $\Gamma_1 + \Gamma_2 + \Gamma_3 = 1$.

T_w can be demonstrated as

$$T_w = T_\infty + T_{ref} b \lambda x (T_w > T_\infty) \tag{6}$$

Where T_{ref} is the reference temperature, u_w is the stretching velocity, and v_f is the kinematic velocity of the base liquid.

The transformations are [59]:

$$\left. \begin{aligned} \psi(x, y) &= \lambda^{\frac{2n-1}{n+1}} v_f^{\frac{1}{n+1}} x^{\frac{2n}{n+1}} f(\eta) \\ u &= x \lambda f', v = -\left(\frac{2n}{n+1}\right) \lambda^{\frac{2n-1}{n+1}} v_f^{\frac{1}{n+1}} x^{\frac{n-1}{n+1}} f, w = x \lambda g, \\ \theta(\eta) &= \frac{T - T_\infty}{T_w - T_\infty}, \eta = \lambda^{\frac{2-n}{n+1}} v_f^{\frac{1}{n+1}} x^{\frac{1-n}{n+1}} y \end{aligned} \right\} \quad (7)$$

$$\left(\frac{\mu_{hnf}}{\mu_f} \right) \left(|g'|^{n-1} g' \right)' + \left(\frac{2n}{n+1} \right) f g' - f' g + \left(\frac{\beta_{hnf}}{\beta_f} \right) K \theta - M \left(\frac{\sigma_{hnf}}{\sigma_f} \right) \left\{ \frac{(1 + \beta_e \beta_i) g - \beta_e f'}{\beta_e^2 + (1 + \beta_e \beta_i)^2} \right\} = 0 \quad (16)$$

$$\left(\frac{k_{hnf}}{(\rho C_p)_{hnf}} \right) \left\{ \frac{1}{Pr_1} (|f'|^{n-1} \theta')' + \frac{1}{Pr_2} (|g'|^{n-1} \theta')' + \frac{1}{Pr_3} (|\theta'|^{n-1} \theta')' \right\} + \left(\frac{2n}{n+1} \right) f \theta' - \eta \left(\frac{1-n}{n+1} \right) f' \theta' - ME_c \left(\frac{\sigma_{hnf}}{(\rho C_p)_{hnf}} \right) \left\{ \frac{(f')^2 + g^2}{\beta_e^2 + (1 + \beta_e \beta_i)^2} \right\} = 0 \quad (17)$$

The velocity components u & v are related with stream function ψ by the relation

$$u = \frac{\partial \psi}{\partial y} \& v = -\frac{\partial \psi}{\partial x} \quad (8)$$

The HNF's thermophysical features are:

$$\frac{\mu_{hnf}}{\mu_f} = (1 - \varphi_1)^{-2.5} (1 - \varphi_2)^{-2.5} \quad (9)$$

$$\frac{\rho_{hnf}}{\rho_f} = (1 - \varphi_2) \left\{ (1 - \varphi_1) + \varphi_1 \left(\frac{\rho_{s_1}}{\rho_f} \right) \right\} + \varphi_2 \left(\frac{\rho_{s_2}}{\rho_f} \right) \quad (10)$$

$$\frac{(\rho C_p)_{hnf}}{(\rho C_p)_f} = (1 - \varphi_2) \left\{ (1 - \varphi_1) + \varphi_1 \left(\frac{(\rho C_p)_{s_1}}{(\rho C_p)_f} \right) \right\} + \varphi_2 \left(\frac{(\rho C_p)_{s_2}}{(\rho C_p)_f} \right) \quad (11)$$

$$\frac{\beta_{hnf}}{\beta_f} = (1 - \varphi_2) \left\{ (1 - \varphi_1) + \varphi_1 \left(\frac{\beta_{s_1}}{\beta_f} \right) \right\} + \varphi_2 \left(\frac{\beta_{s_2}}{\beta_f} \right) \quad (12)$$

$$\frac{\sigma_{hnf}}{\sigma_f} = \left[\frac{\sigma_{s_2} + 2\sigma_{bf} - 2\varphi_2(\sigma_{bf} - \sigma_{s_2})}{\sigma_{s_2} + 2\sigma_{bf} + \varphi_2(\sigma_{bf} - \sigma_{s_2})} \right] \times \left[\frac{\sigma_{s_1} + 2\sigma_f + \varphi_1(\sigma_f - \sigma_{s_1})}{\sigma_{s_1} + 2\sigma_f - 2\varphi_1(\sigma_f - \sigma_{s_1})} \right] \quad (13)$$

$$\frac{k_{hnf}}{k_f} = \left[\frac{k_{s_2} + (m-1)k_{bf} - (m-1)\varphi_2(k_{bf} - k_{s_2})}{k_{s_2} + (m-1)k_{bf} + \varphi_2(k_{bf} - k_{s_2})} \right] \times \left[\frac{k_{s_1} + (m-1)k_f + \varphi_1(k_f - k_{s_1})}{k_{s_1} + (m-1)k_f - (m-1)\varphi_1(k_f - k_{s_1})} \right] \quad (14)$$

Here, the base fluid is Ethylene Glycol while the nanoparticles are Cu&TiO₂.

Using eqs. (6), (7), (9)-(14), eqs. (2)-(5) take the form

$$\left(\frac{\mu_{hnf}}{\mu_f} \right) \left(|f'|^{n-1} f'' \right)' + \left(\frac{2n}{n+1} \right) f f'' - (f')^2 + \left(\frac{\beta_{hnf}}{\beta_f} \right) K \theta - M \left(\frac{\sigma_{hnf}}{\sigma_f} \right) \left\{ \frac{(1 + \beta_e \beta_i) f' - \beta_e g}{\beta_e^2 + (1 + \beta_e \beta_i)^2} \right\} = 0 \quad (15)$$

$$\left. \begin{aligned} f'(0) &= 1, g(0) = 0, f(0) = 0, \\ \frac{k_{hnf}}{k_f} \left\{ \frac{1}{B_{11}} |f'|^{n-1} \theta' + \frac{1}{B_{12}} |g'|^{n-1} \theta' + \frac{1}{B_{13}} |\theta'|^{n-1} \theta' \right\} &= \theta(0) - 1 \\ f'(\infty) &\rightarrow 0, g(\infty) \rightarrow 0, \theta(\infty) \rightarrow 0 \end{aligned} \right\} \quad (18)$$

Here, the non-dimensional parameters are:

$$\left. \begin{aligned} M &= \frac{\sigma_f B_0^2}{\lambda \rho_f}, K = \frac{g \beta_f T_{ref} u_w}{\lambda^2 v_f}, Pr_1 = \frac{v_f}{\Gamma_1 \alpha_f}, Pr_2 = \frac{v_f}{\Gamma_2 \alpha_f}, Pr_4 = \frac{v_f T_{ref}^{1-n} b^{1-n}}{\Gamma_3 \alpha_f}, \\ Bi_1 &= h_f \Gamma_1^{-1} k_f^{-1} \lambda^{\frac{1-2n}{n+1}} v_f^{\frac{n}{n+1}} x^{\frac{1-n}{n+1}}, Bi_2 = h_f \Gamma_2^{-1} k_f^{-1} \lambda^{\frac{1-2n}{n+1}} v_f^{\frac{n}{n+1}} x^{\frac{1-n}{n+1}}, \\ Bi_3 &= h_f \Gamma_3^{-1} k_f^{-1} \lambda^{\frac{1-2n}{n+1}} v_f^{\frac{n}{n+1}} x^{\frac{1-n}{n+1}} b^{1-n} T_{ref}^{-n} \end{aligned} \right\} \quad (19)$$

Where $M, K, Pr_1, Pr_2, Pr_3, Bi_1, Bi_2, Bi_3$ are respectively magnetic parameter, buoyancy parameter, first, second and third modified Prandtl numbers; first, second and third modified Biot numbers respectively.

The skin friction is

$$C_f = \frac{\tau_w}{\frac{1}{2} \rho_{hnf} u_w^2} \quad (20)$$

Where the shear stress,

$$\tau_w = -\mu_{hnf} \left[\frac{\partial u}{\partial y} \right]^{n-1} \frac{\partial u}{\partial y} + \left| \frac{\partial w}{\partial y} \right|^{-(1-n)} \frac{\partial w}{\partial y} \Bigg|_{y=0} \quad (21)$$

In non-dimension,

$$C_f = -2 \left(\frac{\mu_{hnf}}{\mu_f} \right) v_f^{\frac{1}{n+1}} \lambda^{\frac{n-2}{n+1}} x^{\frac{-2}{n+1}} \left(|f''(0)|^{n-1} f''(0) + |g'(0)|^{n-1} g'(0) \right) \quad (22)$$

Here, $|f''(0)|^{n-1} f''(0) + |g'(0)|^{n-1} g'(0)$ is the local skin friction coefficient.

The Nusselt number is

$$Nu_x = \frac{q_w x}{k_{hnf} \left[\Gamma_1 \left| \frac{\partial u}{\partial y} \right|^{n-1} + \Gamma_2 \left| \frac{\partial w}{\partial y} \right|^{n-1} + \Gamma_3 \left| \frac{\partial T}{\partial y} \right|^{n-1} \right] (T_w - T_\infty)} \quad (23)$$

Where $q_w = -k_{hmf} \left[\left(\Gamma_1 \left| \frac{\partial u}{\partial y} \right|^{-(1-n)} + \Gamma_2 \left| \frac{\partial w}{\partial y} \right|^{-(1-n)} + \Gamma_3 \left| \frac{\partial T}{\partial y} \right|^{-(1-n)} \right) \frac{\partial T}{\partial y} \right]_{y=0}$ is

the surface heat flux.

In non-dimension,

$$Nu_x = -\lambda \frac{\partial \theta}{\partial y} \Big|_{y=0} \quad (24)$$

Here, $-\theta'(0)$ is the local Nusselt number.

3. Numerical technique

The governing equations may well be non-linear and coupled and accordingly the MATLAB bvp4c utilized to solve the equations (15) – (17) with the given boundary condition (18). At the initial stage, the boundary value problem written in the form of the IVP and for this purpose, a set of new variables introduced as

$$y = [y_i (i = 1..7)]^T = [f, f', f'', g, g', \theta, \theta']^T \quad (25)$$

and developed governing equation into form of matrix as

$$\begin{pmatrix} y_1 \\ y_2 \\ y_3 \\ y_4 \\ y_5 \\ y_6 \\ y_7 \end{pmatrix} = \begin{pmatrix} y_2 \\ y_3 \\ \left[\frac{2n}{2n+1} y_1 y_3 - y_2^2 + A_3 K y_6 - M \left(\frac{A_3}{A_2} \right) \frac{(1 + \beta_e \beta_i) y_2 - \beta_e y_4}{\beta_e^2 + (1 + \beta_e \beta_i)^2} \right] \\ n \left(\frac{A_1}{A_2} \right) y_3^{n-1} \\ y_5 \\ \left[\frac{2n}{2n+1} y_1 y_5 - y_2 y_4 + A_3 K y_6 - M \left(\frac{A_3}{A_2} \right) \frac{(1 + \beta_e \beta_i) y_4 - \beta_e y_2}{\beta_e^2 + (1 + \beta_e \beta_i)^2} \right] \\ n \left(\frac{A_1}{A_2} \right) y_5^{n-1} \\ y_7 \\ \left(\frac{A_5}{A_6} \right) \left(\frac{n-1}{Pr_1} \right) y_3^{n-2} y_7 \times \\ \left\{ - \frac{2n}{2n+1} y_1 y_3 - y_2^2 + A_3 K y_6 - M \left(\frac{A_3}{A_2} \right) \frac{(1 + \beta_e \beta_i) y_2 - \beta_e y_4}{\beta_e^2 + (1 + \beta_e \beta_i)^2} \right\} \\ n \left(\frac{A_1}{A_2} \right) y_3^{n-1} \\ \left(\frac{A_5}{A_6} \right) \left(\frac{n-1}{Pr_2} \right) y_5^{n-2} \times \\ \left\{ - \frac{2n}{2n+1} y_1 y_5 - y_2 y_4 + A_3 K y_6 - M \left(\frac{A_3}{A_2} \right) \frac{(1 + \beta_e \beta_i) y_4 - \beta_e y_2}{\beta_e^2 + (1 + \beta_e \beta_i)^2} \right\} \\ n \left(\frac{A_1}{A_2} \right) y_5^{n-1} \\ + \frac{2n}{2n+1} y_1 y_7 - \eta \left(\frac{1-n}{1+n} \right) y_2 y_7 - ME_c \left(\frac{A_4}{A_6} \right) \frac{y_2^2 + y_4^2}{\beta_e^2 + (1 + \beta_e \beta_i)^2} \\ \left(\frac{A_5}{A_6} \right) \left\{ \frac{1}{Pr_1} y_3^{n-1} + \frac{1}{Pr_2} y_5^{n-1} + \frac{n}{Pr_3} y_7^{n-1} \right\} \end{pmatrix}, \quad (26)$$

with

$$(A_1, A_2, A_3, A_4, A_5, A_6) = \left(\frac{\mu_{hmf}}{\mu_f}, \frac{\rho_{hmf}}{\rho_f}, \frac{\beta_{hmf}}{\beta_f}, \frac{\sigma_{hmf}}{\sigma_f}, \frac{k_{hmf}}{k_f}, \frac{(\rho c_p)_{hmf}}{(\rho c_p)_f} \right)$$

At $\eta = 0$, conditions are written as

$$y(0) = \left[0, 1, I_1, 0, I_2, 1 + A_5 \left\{ \frac{1}{Bi_1} I_1^{n-1} I_3 + \frac{1}{Bi_2} I_2^{n-1} I_3 + \frac{1}{Bi_3} I_3^n \right\}, I_3 \right] \quad (27)$$

With unknown constants I_1, I_2 and I_3 .

Shooting approach would be utilized to get an initial assumption of the unknown parameters at the initial guess and then considered MATLAB's ODE solver is utilized to solve the matrix in equation (26) with the initial condition (see Eq. (27)).

Defined the convergence criteria with error $|E_i| < \text{tolerance} = 10^{-10}$ where:

$$\begin{aligned} E_1 &= y_3(\infty, I_1) - f'(\infty), \\ E_2 &= y_3(\infty, I_2) - g'(\infty), \\ E_3 &= y_5(\infty, I_3) - \theta(\infty). \end{aligned} \quad (28)$$

In this work, $\eta(\eta_\infty)$ is assumed to have an utmost amount of 10.

4. Validation

Present outcomes of $f''(0)$ were compared with the work of Bachok

et al. [60] and Si et al. [61] under some constraints and it observed that the outcomes are significantly similar to their results. Results are observed in Table 4, and they give us confidence in the accuracy of our numerical analysis and the outcomes of our current work.

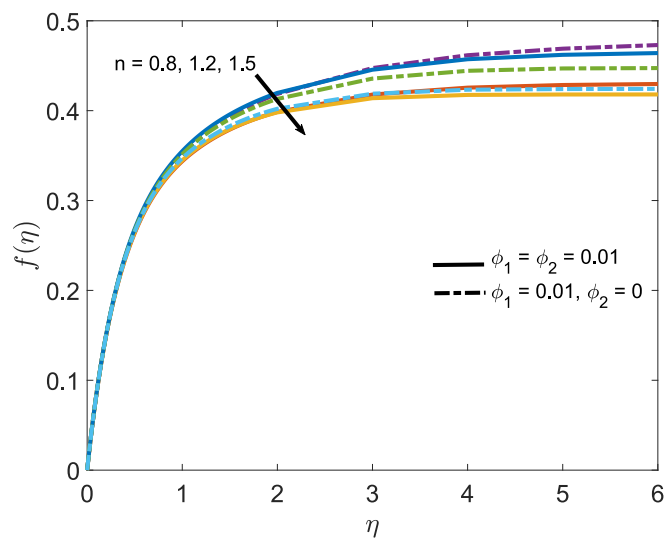


Fig. 2a. Role of $f(\eta)$ with n .

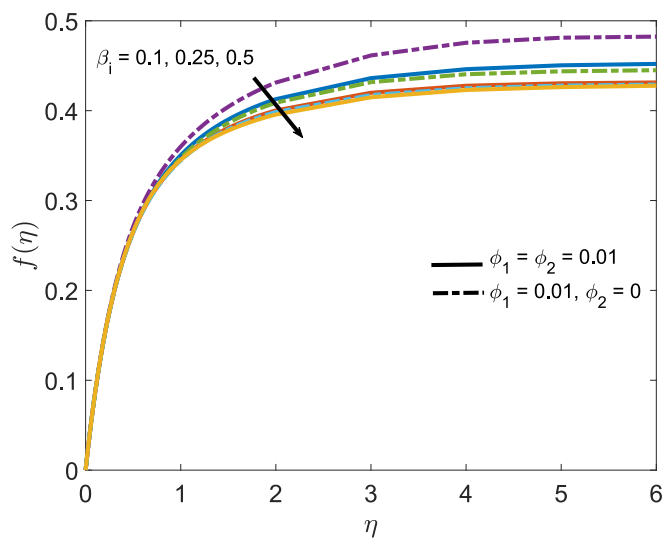


Fig. 2d. Role of $f(\eta)$ with β_i .

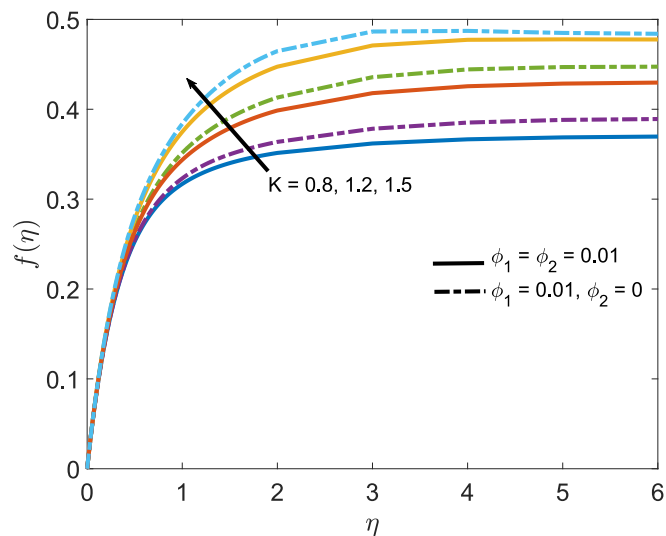


Fig. 2b. Role of $f(\eta)$ with K .

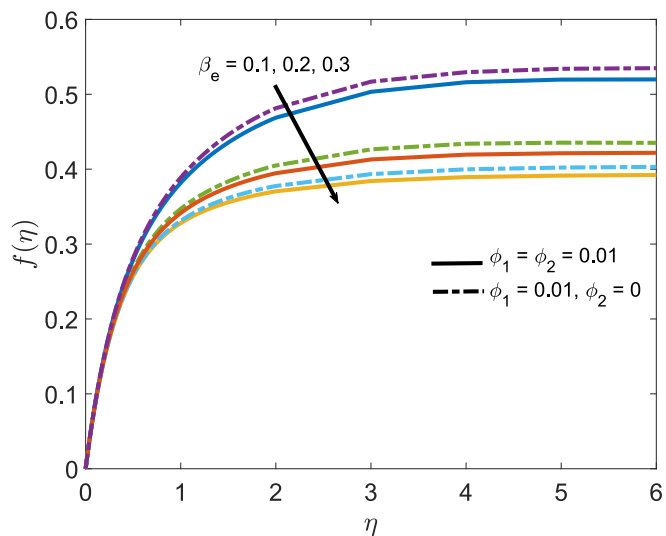


Fig. 2e. Role of $f(\eta)$ with β_e .

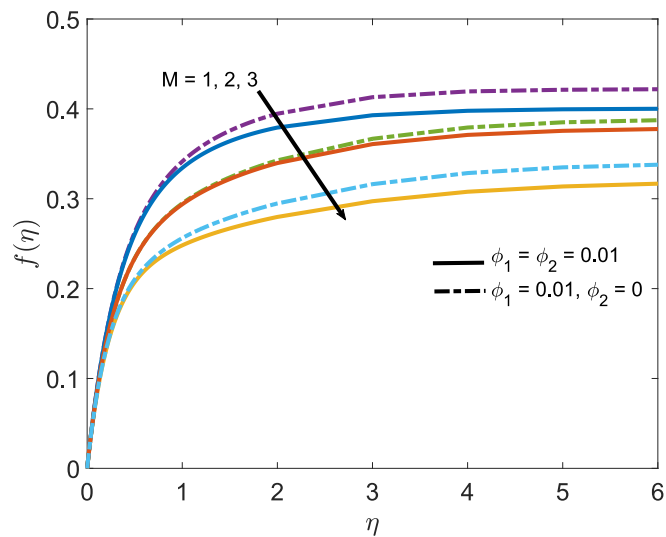


Fig. 2c. Role of $f(\eta)$ with M .

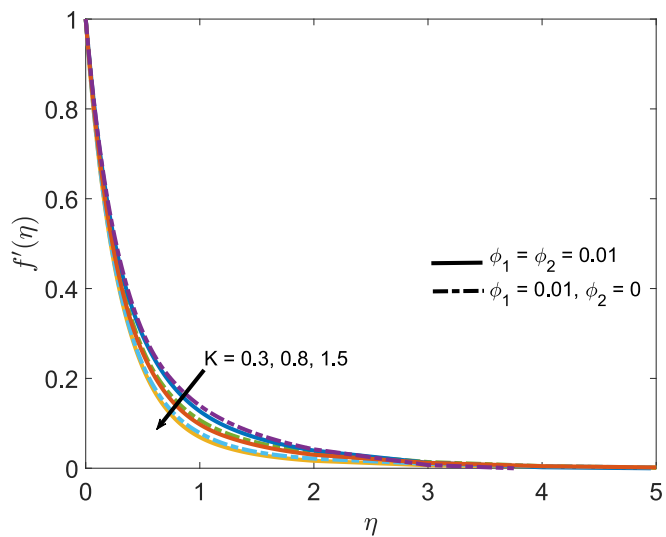


Fig. 3a. Role of $f'(\eta)$ with K .

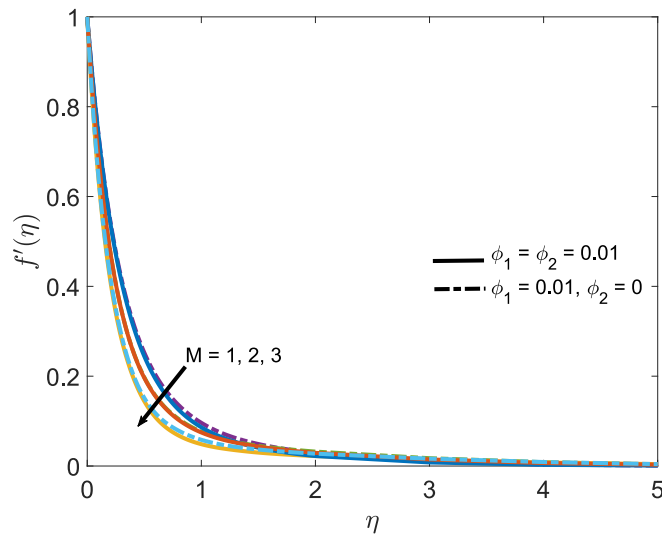


Fig. 3b. Role of $f'(\eta)$ with M .

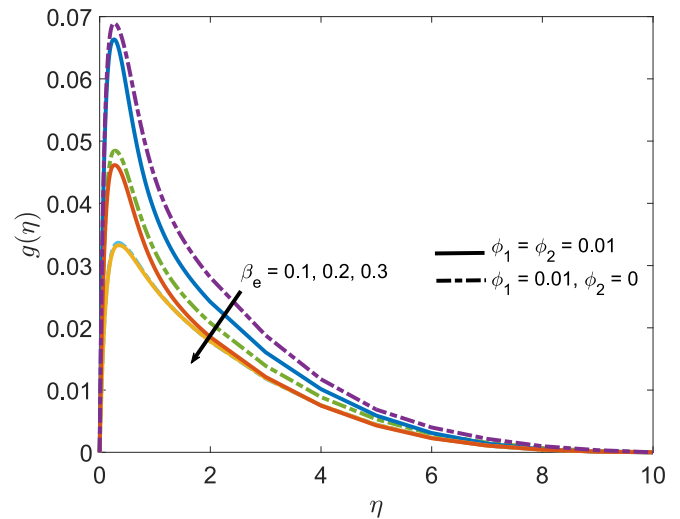


Fig. 4b. Role of $g(\eta)$ with β_e .

5. Results and discussion

In this part, the efficacy of various pertinent parameters on the flow and thermal behavior of PLF with hybrid nanostructure ($Cu + TiO_2 + EG$) over a stretched sheet subject to modified Fourier's law are discussed. The range of parameters chosen is that power law index ($0.8 \leq n \leq 1.5$), buoyancy parameter ($0.3 \leq K \leq 1.5$), magnetic parameter ($1 \leq M \leq 3$), Hall parameter ($0.1 \leq \beta_i \leq 0.5$), ion slip parameter ($0.1 \leq \beta_e \leq 0.3$), first modified Prandtl number ($1 \leq Pr_1 \leq 3$), second modified Prandtl number ($1 \leq Pr_2 \leq 3$), third modified Prandtl number ($1 \leq Pr_3 \leq 3$), first modified Biot number ($1 \leq Bi_1 \leq 3$), second modified Biot number ($1 \leq Bi_2 \leq 3$), and third modified Biot number ($1 \leq Bi_3 \leq 3$). The power-law hybrid nanofluid (PLHNF) ($\phi_1 = \phi_2 = 0.01$) is represented by solid line and power-law nanofluid (PLNF) ($\phi_1 = 0.01, \phi_2 = 0$) is represented by dotted line in the graphs developed.

5.1. Analysis of velocity profile

Fig. 2a shows the influence of n on the transverse velocity $f(\eta)$. The $f(\eta)$ takes suddenly higher value near the wall and converges slowly with the increasing value of η . Further, $f(\eta)$ peters out with rise in n for both PLHNF and PLNF. Physically, amplification of n indicates the

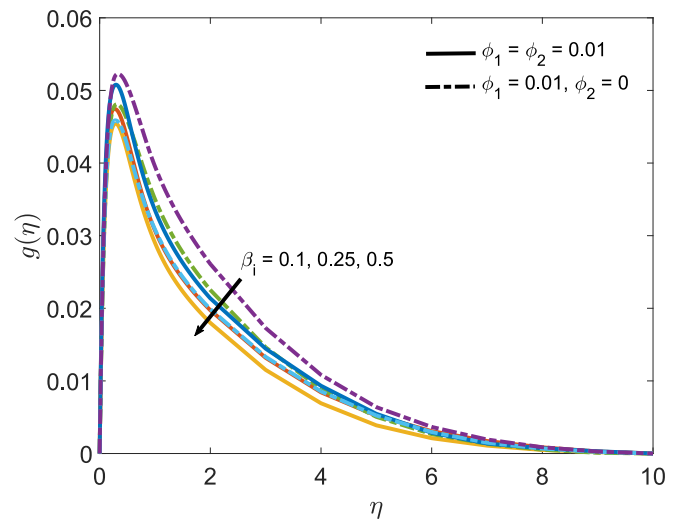


Fig. 4c. Role of $g(\eta)$ with β_i .

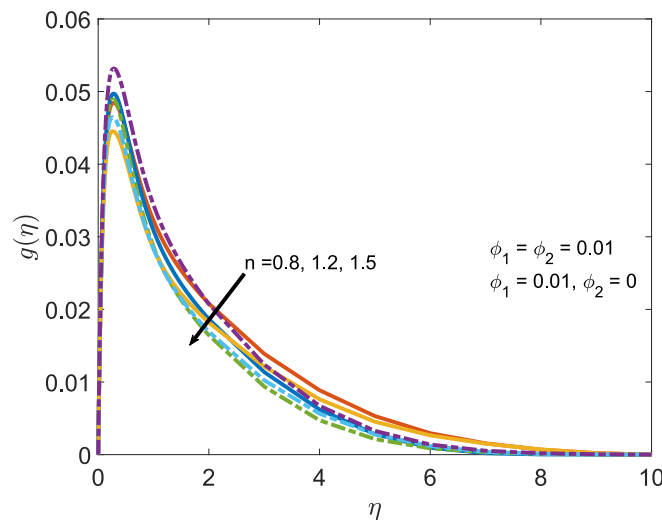


Fig. 4a. Role of $g(\eta)$ with n .

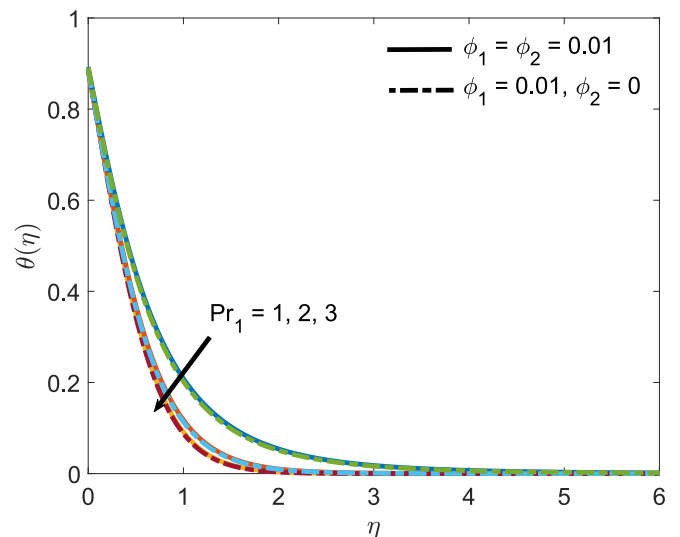


Fig. 5a. Role of $\theta(\eta)$ with Pr_1 .

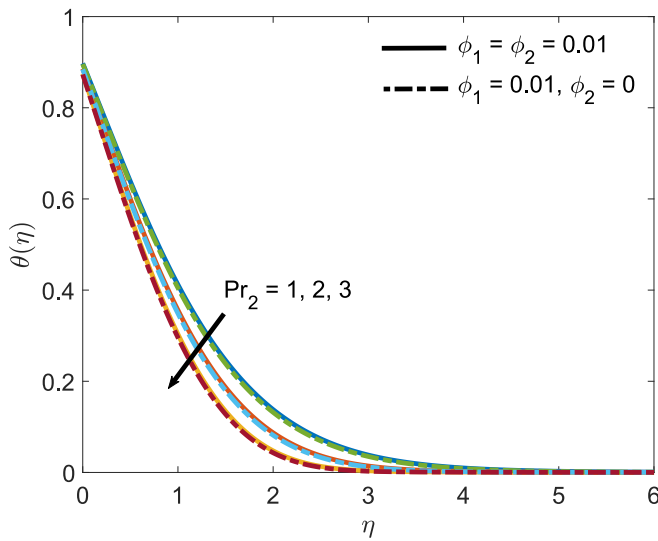


Fig. 5b. Role of $\theta(\eta)$ with Pr_2 .

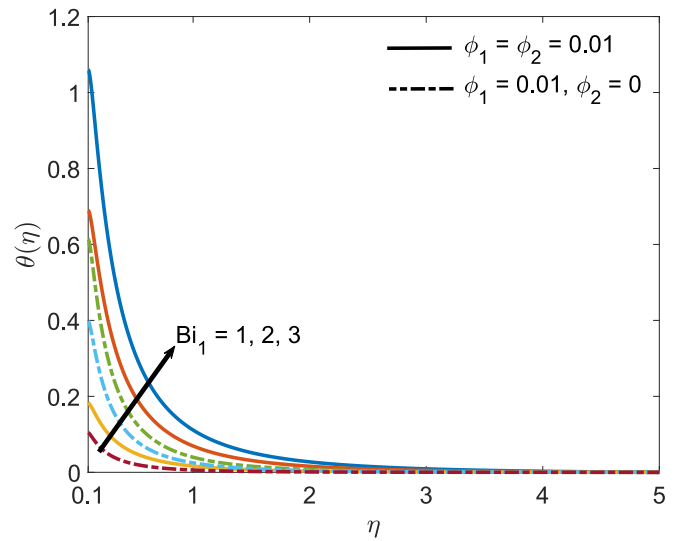


Fig. 6a. Role of $\theta(\eta)$ with Bi_1 .

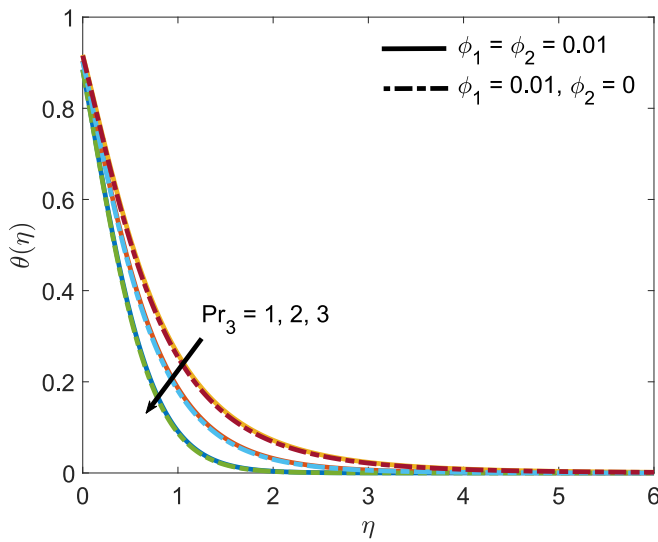


Fig. 5c. Role of $\theta(\eta)$ with Pr_3 .

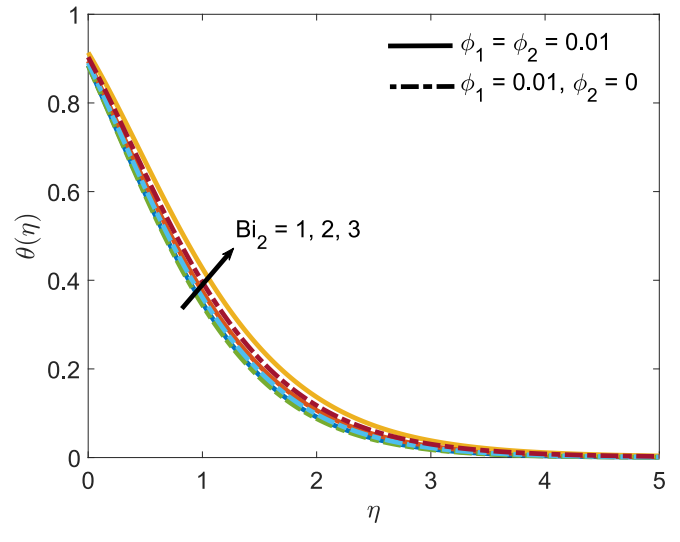


Fig. 6b. Role of $\theta(\eta)$ with Bi_2 .

intensification of viscosity of PLHNF thereby enhancing its velocity. However, at fixed η , $f(\eta)$ is higher for PLNF than PLHNF in the flow domain. This is because the viscosity of PLNF is lower than that of PLHNF. Fig. 2b displays that $f(\eta)$ takes suddenly higher value near the wall and after that converges slowly with increasing value of η whatever the values of buoyancy parameter K . Further, $f(\eta)$ of both PLHNF and PLNF ameliorates with rise in K as we recede from the surface of the stretched sheet. This is because greater K indicates greater buoyancy force thereby raising the fluid (PLHNF/PLNF) up with greater velocity against viscous shear. At fixed K , $f(\eta)$ of PLNF is greater than that of PLHNF. The $f(\eta)$ shows whittles down with rise in magnetic parameter M ($M = 1, 2, 3$) for both PLHNF and PLNF which is exactly opposite to that of K as illustrated in Fig. 2c. In fact, Lorentz force created by the applied magnetic field subject to conducting PLHNF and PLNF impedes their motion. At particular strength of magnetic field (at fixed M), $f(\eta)$ of PLNF exceeds than that of PLHNF. Figs. 2d and 2e visualize the influence of β_i and β_e on $f(\eta)$ for both PLHNF and PLNF. Amplification of both β_i and β_e accounts for the emaciation of $f(\eta)$ for both PLHNF and PLNF. Indeed, the interaction among fluid plasma and applied magnetic field may well be responsible for the development of Hall and ion forces. When β_i and β_e rise, Hall and ion forces increase thereby indicating more

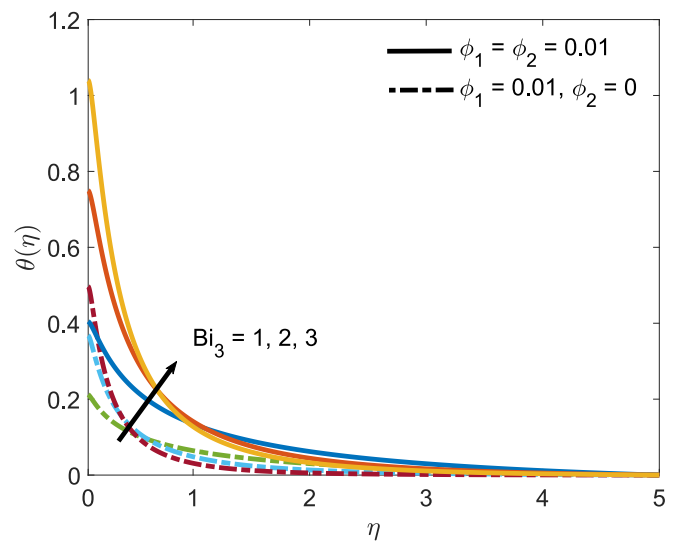


Fig. 6c. Role of $\theta(\eta)$ with Bi_3 .

Table 2
Impact of local skin friction coefficients for varying parameters with a comparison between PLHNF and PLNF.

| M | n | K | Pr ₁ | Pr ₂ | Pr ₃ | Ec | β _i | β _e | f'(0) ⁿ⁻¹ f'(0) + g'(0) ⁿ⁻¹ g'(0) | |
|--------|--------|--------|-----------------|-----------------|-----------------|--------|----------------|----------------|--|---|
| | | | | | | | | | φ ₁ = 0.01φ ₂ = 0.01 | φ ₁ = 0.01φ ₂ = 0.0 |
| 123 | 1.2 | 0.8 | 1 | 1 | 1 | 0.1 | 0.2 | 0.2 | -1.9714761 | -2.0219993 |
| | | | | | | | | | -2.3785182 | -2.3816112 |
| | | | | | | | | | -2.8256935 | -2.8679898 |
| | 0.81.5 | 1.52 | 23 | 23 | 0.10.4 | 0.20.3 | 0.10.5 | 0.10.5 | -1.8805028 | -1.7257652 |
| | | | | | | | | | -2.0842258 | -2.0557487 |
| | | | | | | | | | -1.6286608 | -1.6734424 |
| | 0.10.5 | 0.10.5 | 0.10.5 | 0.10.5 | 0.10.5 | 0.10.5 | 0.10.5 | 0.10.5 | -1.3921195 | -1.3837419 |
| | | | | | | | | | -1.8655198 | -1.8945101 |
| | | | | | | | | | -1.9149459 | -1.9726605 |
| | 0.10.5 | 0.10.5 | 0.10.5 | 0.10.5 | 0.10.5 | 0.10.5 | 0.10.5 | 0.10.5 | -1.9242273 | -1.9336412 |
| | | | | | | | | | -1.9537642 | -1.9582206 |
| | | | | | | | | | -1.8880616 | -1.8649800 |
| | 0.10.5 | 0.10.5 | 0.10.5 | 0.10.5 | 0.10.5 | 0.10.5 | 0.10.5 | 0.10.5 | -1.9060930 | -1.9530697 |
| | | | | | | | | | -1.9367585 | -1.9383570 |
| | | | | | | | | | -1.8506439 | -1.9005737 |
| 0.10.5 | 0.10.5 | 0.10.5 | 0.10.5 | 0.10.5 | 0.10.5 | 0.10.5 | 0.10.5 | -1.9845783 | -2.0380438 | |
| | | | | | | | | -1.9521967 | -1.9581721 | |
| | | | | | | | | -2.1733159 | -2.1892795 | |
| 0.10.5 | 0.10.5 | 0.10.5 | 0.10.5 | 0.10.5 | 0.10.5 | 0.10.5 | 0.10.5 | -1.2082555 | -1.2785637 | |

Table 3
Impact of local heat transfer rate for varying parameters with a comparison between PLHNF and PLNF.

| M | n | K | Pr ₁ | Pr ₂ | Pr ₃ | Ec | β _i | β _e | -θ'(0) | |
|--------|--------|--------|-----------------|-----------------|-----------------|--------|----------------|----------------------|--|---|
| | | | | | | | | | φ ₁ = 0.01φ ₂ = 0.01 | φ ₁ = 0.01φ ₂ = 0.0 |
| 123 | 1.2 | 0.8 | 1 | 1 | 1 | 0.1 | 0.2 | 0.2 | 0.502671050.408779530.17748790 | |
| | | | | | | | | | 0.776020860.41306269 | |
| | | | | | | | | | 0.507296830.49114046 | |
| | 0.81.5 | 1.52 | 23 | 23 | 0.10.4 | 0.20.3 | 0.10.5 | 0.10.5 | 0.484041400.37262718 | |
| | | | | | | | | | 0.507499110.40128883 | |
| | | | | | | | | | 0.323892520.31983137 | |
| | 0.10.5 | 0.10.5 | 0.10.5 | 0.10.5 | 0.10.5 | 0.10.5 | 0.10.5 | 0.10.5 | 0.373265310.27134041 | |
| | | | | | | | | | 0.288869820.56552985 | |
| | | | | | | | | | 0.532080210.36280345 | |
| | 0.10.5 | 0.10.5 | 0.10.5 | 0.10.5 | 0.10.5 | 0.10.5 | 0.10.5 | 0.10.5 | 0.501282230.407732380.17221110 | |
| | | | | | | | | | 0.766235630.40047227 | |
| | | | | | | | | | 0.506170090.49657900 | |
| | 0.10.5 | 0.10.5 | 0.10.5 | 0.10.5 | 0.10.5 | 0.10.5 | 0.10.5 | 0.10.5 | 0.476038020.36947580 | |
| | | | | | | | | | 0.490125890.39427396 | |
| | | | | | | | | | 0.319380700.30456065 | |
| 0.10.5 | 0.10.5 | 0.10.5 | 0.10.5 | 0.10.5 | 0.10.5 | 0.10.5 | 0.10.5 | 0.330525690.23629919 | | |
| | | | | | | | | 0.272067350.52802380 | | |
| | | | | | | | | 0.529818360.36098439 | | |

Table 4
Comparison of f'(0) with the previous works of Bachok et al. [60] and Si et al. [61] for φ₂ = 0 = K = M = Ec, n = 1, ε = 1, Pr₁ = 6.7, Pr₂, Pr₃ → ∞, Bi₁, Bi₂, Bi₂ → ∞.

| φ ₂ | f'(0) | | |
|----------------|--------------------|----------------|-------------|
| | Bachok et al. [60] | Si et al. [61] | Present |
| 0 | -0.4438 | -0.443762 | -0.44375821 |
| 0.1 | -0.5218 | -0.521295 | -0.52129431 |
| 0.2 | -0.5405 | -0.540537 | -0.54053682 |

applied magnetic field yielding greater Lorentz force. Consequently, velocity of PLHNF and PLNF diminishes.

The variation of primary velocity, f'(η) for different K (K = 0.3, 0.8, 1.5) for both HNF and MNF is shown in Fig. 3a. It is seen that f'(η) may peter out with amplification in K for both HNF and MNF. In fact, rise in K enhances horizontal velocity. As a result the flow would be decelerated along axial direction. At fixed K (say, K = 0.3), f'(η) for MNF is slightly greater than that of HNF. Further, f'(η) whittles down with rise in M (M = 1, 2, 3) for both HNF and MNF as illustrated in Fig. 3b. At fixed M, f'(η) for MNF is slightly greater than that of HNF. It is due to the Lorentz force that hinders the fluid movement.

The secondary velocity g(η) reduces with rise in power-law-index n (n = 0.8, 1.2, 1.5) for both HNF and MNF (Fig. 4a). At fixed n (say n = 0.8), g(η) for PLNF is greater than that of PLHNF. Consideration of HNF leads to the greater viscosity compared to MNF. As a result, g(η) decays. Amplification in power-law index results in greater viscosity of

PLHNF and HNF thereby emaciating their velocity. Fig. 4b indicates that rise in β_e (β_e = 0.1, 0.2, 0.3) accounts for the diminution of g(η) for both PLHNF and PLNF. At fixed β_e (say, β_e = 0.1), it is visualized that g(η) attains larger value for PLNF than PLHNF. Exactly same behavior is envisaged for different β_i (β_i = 0.1, 0.25, 0.5) as portrayed in Fig. 4c. Some overshoots appear nearby the solid boundary. This is because fluid velocity near the solid boundary is greater than that of ambient fluid.

5.2. Analysis of temperature profile

Figs. 5a–5c indicate that the fluid temperature θ(η) decreases with rise in first modified Prandtl number Pr₁ (Pr₁ = 1, 2, 3), second modified Prandtl number Pr₂ (Pr₂ = 1, 2, 3), third modified Prandtl number Pr₃ (Pr₃ = 1, 2, 3) for both PLHNF and PLNF. The θ(η) variation is prominent. Physically, amplifying modified Prandtl numbers accounts for the diminution of thermal diffusivity thereby decreasing the heat propagation into the flow domain. As a result, θ(η) gets reduced. Figs. 6a–6c reveal that θ(η) uplifts effectively due to rise in first modified Biot number, Bi₁ (Bi₁ = 1, 2, 3), second modified Biot number Bi₂ (Bi₂ = 1, 2, 3), third modified Biot number Bi₃ (Bi₃ = 1, 2, 3) for both PLHNF and PLNF. Indeed, rise in Biot number leads to the greater convective heating below the surface of the stretched sheet thereby lifting up the fluid temperature within the boundary layer and the corresponding thermal boundary layers' thickness.

5.3. Analysis of Nusselt number and skin friction profiles

The alteration of skin friction coefficient for different values of pa-

parameters $M, n, K, Pr_1, Pr_2, Pr_3, Ec, \beta_i, \beta_e$ is shown in Table 2. It is seen that amplification of $M, n, K, Pr_1, Pr_2, Pr_3, Bi$ enhances skin friction while reverse effect is obtained with rise in K, Ec, β_e for both PLHNF and PLNF. The Nu variation for varying amounts of parameters like $M, n, K, Pr_1, Pr_2, Pr_3, Ec, \beta_i, \beta_e$ for both PLHNF and PLNF is mentioned in Table 3. It is visualized that Nu whittles down with rise in $M, K, Pr_1, Pr_2, Pr_3, Ec, \beta_e$ while opposite trend is obtained with rise in β_i .

6. Conclusions

The principal investigation of the this research is to dissect Hall and ion-slip efficacy on thermo-fluidic flow of magnetic power-law HNF using modified Fourier's law featured with velocity and temperature gradients. The major outcomes are:

- The velocity $f'(\eta)$ peters out with rise in n, M, K for both PLHNF and PLNF.
- Amplification of both β_i and β_e accounts for the emaciation of $f(\eta)$ for both PLHNF and PLNF.
- Amplifying modified Prandtl numbers Pr_1, Pr_2, Pr_3 accounts for the uplift of $\theta(\eta)$ while that of modified Biot numbers Bi_1, Bi_2, Bi_3 exhibits reverse effect
- Amplification of $M, n, K, Pr_1, Pr_2, Pr_3, Bi$ enhances skin friction while reverse effect is obtained with rise in K, Ec, β_e for both PLHNF and PLNF.
- Nusselt number whittles down with rise in $M, K, Pr_1, Pr_2, Pr_3, Ec, \beta_e$ while opposite trend is obtained with rise in β_i .

7. Limitation

The sedimentation of hybrid nanoparticles in hybrid nanofluid and stability issue are the limitations of the present investigation.

8. Future perspective

The current work can be extended by replacing hybrid nanofluid by ternary hybrid nanofluid (mixture of three different nanoparticles and base fluid) in order to achieve more stable heat transfer power-law fluid thereby imparting greater cooling in industrial thermal systems. In ternary hybrid nanofluid, the choice of nanoparticles should be graphene (very high thermal and electrical conductivities), alumina (more stability) and TiO_2 (dielectric properties, high thermal conductivity, photo catalytic activities, and low cost). Further, Darcy-Forchheimer medium can be implemented in order to accomplish prominent heat transfer rate from the desired thermal systems.

CRedit authorship contribution statement

N. Sultana: Investigation, Formal analysis, Writing. **S. Shaw:** Methodology, Investigation, Software. **S. Mondal:** Conceptualization, Formal Analysis, Methodology. **M.K. Nayak:** Methodology, Writing, Supervision, Validation. **S. Nazari:** Conceptualization, Formal analysis, Investigation. **A. Mouldi:** Writing, Formal analysis. **A.J. Chamkha:** Investigation, Supervision.

Declaration of competing interest

The authors declare that they have no known competing financial interests or personal relationships that could have appeared to influence the work reported in this paper.

Acknowledgement

The authors extend their appreciation to the Deanship of Scientific Research at King Khalid University for funding this work through

research groups under grant number RGP2/126/44.

References

- [1] Crane LJ. Flow past a stretching plate. *J Appl Math Phys* 1970;21:645–7.
- [2] Wang CY. Three-dimensional flow due to a stretching flat surface. *Phys Fluids* 1984;27:1915–7.
- [3] Lakshminisha KN, Venkateswaran S, Nath G. Three-dimensional unsteady flow with heat and mass transfer over a continuous stretching surface. *ASME J Heat Transf* 1988;110:590–5.
- [4] Takhar HS, Chamkha AJ, Nath G. Unsteady three-dimensional MHD boundary layer flow due to the impulsive motion of a stretching surface. *Acta Mech* 2001; 146:59–71.
- [5] Mukhopadhyay S, Gorla RSR. Unsteady MHD boundary layer flow of an upper convected maxwell fluid past a stretching sheet with first order constructive/ destructive chemical reaction. *J Nav Archit Mar Eng* 2012;9(2).
- [6] Mukhopadhyay S, Arif MG, Ali Pk MW. Effects of transpiration on unsteady MHD flow of an upper convected Maxwell (UCM) fluid passing through a stretching surface in the presence of a first order chemical reaction. *Chin Phys B* 2013;22(12): 124701.
- [7] Mukhopadhyay S. Upper-convected Maxwell fluid flow over an unsteady stretching surface embedded in porous medium subjected to suction/blowing. *Zeitschrift Für Naturforschung A* 2012;67(10–11):641–6.
- [8] Vajravelu K, Mukhopadhyay S. Fluid flow, heat and mass transfer at bodies of different shapes: Numerical solutions. Academic Press; 2015.
- [9] Mandal IC, Mukhopadhyay S. Nonlinear convection in micropolar fluid flow past a non-isothermal exponentially permeable stretching sheet in presence of heat source/sink. *Therm Eng* 2020;67:202–15.
- [10] Mukhopadhyay S, Vajravelu K. Effects of transpiration and internal heat generation/absorption on the unsteady flow of a Maxwell fluid at a stretching surface. *J Appl Mech* 2012;79(4):044508.
- [11] Mukhopadhyay S, Bhattacharyya K, Layek GC. Mass transfer over an exponentially stretching porous sheet embedded in a stratified medium. *Chem Eng Commun* 2014;201(2):272–86.
- [12] Mukhopadhyay S, Mondal IC, Gorla RSR. Effects of thermal stratification on flow and heat transfer past a porous vertical stretching surface. *Heat Mass Transf* 2012; 48:915–21.
- [13] Bhattacharyya K, Mukhopadhyay S, Layek GC. Effects of partial slip on boundary layer stagnation-point flow and heat transfer towards a stretching sheet with temperature dependent fluid viscosity. *Acta Tech* 2012;57(2):183–95.
- [14] Mukhopadhyay S. Chemically reactive solute transfer in a boundary layer slip flow along a stretching cylinder. *Front Chem Sci Eng* 2011;5:385–91.
- [15] Lamsaadi M, Naïmi M, Hasnaoui M. Natural convection of non-Newtonian power law fluids in a shallow horizontal rectangular cavity uniformly heated from below. *Heat Mass Transf* 2005;41:239–49.
- [16] Usman P, Lin A, Ghaffari, Steady flow and heat transfer of the power-law fluid between two stretchable rotating disks with non-uniform heat source/sink. *J Therm Anal Calorim* 2021;146:1735–49.
- [17] Haldar S, Mukhopadhyay S, Layek GC. Dual solutions of Casson fluid flows over a power-law stretching sheet. *J Appl Mech Tech Phys* 2017;58:629–34.
- [18] Mukhopadhyay S, Andersson HI. Shear flow of a Newtonian fluid over a quiescent generalized Newtonian fluid. *Meccanica* 2017;52:903–14.
- [19] Sadeghi MS, Tayebi T, Dogonchi AS, Nayak MK, Waqas M. Analysis of thermal behavior of magnetic buoyancy-driven flow in ferrofluid-filled wavy enclosure furnished with two circular cylinders. *Int Commun Heat Mass Transfer* 2021;120: 104951.
- [20] Nayak MK. Chemical reaction effect on MHD viscoelastic fluid over a stretching sheet through porous medium. *Meccanica* 2016;51:1699–711.
- [21] Nayak MK, Dash GC, Singh LP. Heat and mass transfer effects on MHD viscoelastic fluid over a stretching sheet through porous medium in presence of chemical reaction. *Propul Power Res* 2016;5(1):70–80.
- [22] Nayak MK, Dash GC, Singh LP. Steady MHD flow and heat transfer of a third grade fluid in wire coating analysis with temperature dependent viscosity. *Int J Heat Mass Transf* 2014;79:1087–95.
- [23] Choi SUS. Enhancing thermal conductivity of fluids with nanoparticles. *ASME Fluids Eng Division* 1995;231:99–105.
- [24] Eastman JA, Choi SUS, Li S, Yu W, Thompson LJ. Anomalous increased effective thermal conductivities of ethylene glycol-based nanofluids containing copper nanoparticles. *Appl Phys Lett* 2001;78:718–20.
- [25] Xie HQ, Lee H, Youn W, Choi M. Nanofluids containing multi-walled carbon nanotubes and their enhanced thermal conductivities. *J Appl Phys* 2003;94: 4967–71.
- [26] Ghosh S, Mukhopadhyay S. Flow and heat transfer of nanofluid over an exponentially shrinking porous sheet with heat and mass fluxes. *Propul Power Res* 2018;7(3):268–75.
- [27] Abbas N, Nadeem S, Saleem A. Computational analysis of water based Cu-Al₂O₃ /H₂O flow over a vertical wedge. *Adv Mech Eng* 2020;12(11). <https://doi.org/10.1177/1687814020968322>.
- [28] Abbas N, Rehman KU, Shatanawi W, Abodayeh K. Mathematical model of temperature-dependent flow of power-law nanofluid over a variable stretching Riga sheet. *Waves Random Complex Media* 2022;1–18. <https://doi.org/10.1080/17455030.2022.2111029>.
- [29] Awan AU, Abid S, Abbas N. Theoretical study of unsteady oblique stagnation point based Jeffrey nanofluid flow over an oscillatory stretching sheet. *Adv Mech Eng* 2020;12(11). <https://doi.org/10.1177/1687814020971881>.

- [30] Abbas N, Shatanawi W, Rehman KU, Shatanawi TA. Velocity and thermal slips impact on boundary layer flow of micropolar nanofluid over a vertical nonlinear stretched Riga sheet, *Proc Inst Mech Eng, Part N: J Nanomater, Nanoeng Nanosyst*, (2023) <https://doi.org/10.1177/23977914231156685>.
- [31] Nayak MK, Agbaje TM, Mondal S, Sibanda P, Leach PGL. Thermodynamic effect in Darcy-Forchheimer nanofluid flow of a single-wall carbon nanotube/multi-wall carbon nanotube suspension due to a stretching/shrinking rotating disk. *J Eng Math* 2020;120:43–65.
- [32] Nayak MK, Mehmood R, Muhammad T, Khan AU, Waqas H. Entropy minimization in mixed convective Falkner-Skan flow of ZnO-SAE50 nanolubricant over stationary/moving Riga plate. *Case Stud Therm Eng* 2021;26:101176.
- [33] Nayak MK, Oyelakin IS, Chamkha AJ, Mondal S, Sibanda P. Three-dimensional rotating flow of an Oldroyd-B nanofluid with relaxation-retardation viscous dissipation. *J Nanofluids* 2021;10(3):408–19.
- [34] Nayak MK, Oloniju SD, Mondal S, Goqo SP, Sibanda P. Flow and heat transfer over a thin needle immersed in a porous medium filled with an Al₂O₃-water nanofluids using Buongiorno's two-phase model. *Int J Ambient Energy* 2022;43(1):3652–60.
- [35] Sultana N, Shaw S, Nayak MK, Mondal S. Hydromagnetic slip flow and heat transfer treatment of Maxwell fluid with hybrid nanostructure: low Prandtl numbers. *Int J Ambient Energy* 2023;44(1):947–57.
- [36] Ranga Babu JA, Kumar KK, Rao SS. State-of-art review on hybrid nanofluids. *Renew Sustain Energy Rev* 2017;77:551–65.
- [37] Cimpean DS, Sheremet MA, Pop I. Mixed convection of hybrid nanofluid in a porous trapezoidal chamber. *Int Commun Heat Mass Tran* 2020;116:104627.
- [38] Sadiq MA. Non-Fourier heat transfer enhancement in power law fluid with mono and hybrid nanoparticles. *Sci Rep* 2021;11:20919.
- [39] Zeeshan NA, Ahammad NA, Shah JDC. Role of nanofluid and hybrid nanofluid for enhancing thermal conductivity towards exponentially stretching curve with modified Fourier law inspired by melting heat effect. *Math* 2023;11(5). 1170 (1–21).
- [40] Gope R, Nayak MK, Shaw S, Mondal S. Hydro-thermo-fluidic aspects of Oldroyd B fluid with hybrid nanostructure subject to low and moderate Prandtl numbers. *Multidiscip Model Mater Struct* 2023;19(2):292–310.
- [41] Shao Y, Nayak MK, Dogonchi AS, Chamkha AJ, Elmasry Y, Galal AM. Ternary hybrid nanofluid natural convection within a porous prismatic enclosure with two movable hot baffles: An approach to effective cooling. *Case Stud Therm Eng* 2022; 40:102507.
- [42] Nayak MK, Karimi N, Chamkha AJ, Dogonchi AS, El-Sapa S, Galal AM. Efficacy of diverse structures of wavy baffles on heat transfer amplification of double-diffusive natural convection inside a C-shaped enclosure filled with hybrid nanofluid. *Sustain Energy Technol Assess* 2022;52:102180.
- [43] Shaw S, Samantaray SS, Misra A, Nayak MK, Makinde OD. Hydromagnetic flow and thermal interpretations of Cross hybrid nanofluid influenced by linear, nonlinear and quadratic thermal radiations for any Prandtl number. *Int Commun Heat Mass Transfer* 2022;130:105816.
- [44] Nayak MK, Shaw S, Waqas H, Muhammad T. Numerical computation for entropy generation in Darcy-Forchheimer transport of hybrid nanofluids with Cattaneo-Christov double-diffusion. *Int J Numer Methods Heat Fluid Flow* 32 (6) 1851-1882.
- [45] Cheng CY. Combined heat and mass transfer in natural convection flow from a vertical wavy surface in a power-law fluid saturated porous medium with thermal and mass stratification. *Int Commun Heat Mass Transf* 2009;36(4):351–6.
- [46] Mahapatra TR, Mondal S, Pal D. Heat transfer due to magnetohydrodynamic stagnation-point flow of a power-law fluid towards a stretching surface in the presence of thermal radiation and suction/injection. *ISRN Thermodynamics* 2012; 2012:465864.
- [47] Abbas N, Shatanawi W, Abodayeh K. Computational analysis of MHD nonlinear radiation casson hybrid nanofluid flow at vertical stretching sheet. *Symmetry* 2022;14(7):1494.
- [48] Abbas N, Shatanawi W, Shatanawi TA. Numerical approach for induced MHD Sutterby fluid flow with variable thermal conductivity over a stretching cylinder. *Case Studi Therm Eng* 2023;49:103163.
- [49] Ghosh S, Mukhopadhyay S. Unsteady MHD three-dimensional flow of nanofluid over a stretching surface with zero nanoparticles flux and thermal radiation. *Waves Random Complex Media* 2021:1–17.
- [50] Nazarov YV. Generalized Ohm's Law. In: Cerdeira, H.A., Kramer, B., Schön, G. (eds) *Quantum Dynamics of Submicron Structures*, NATO ASI Series, Springer, Dordrecht. 291 (1995) 687–704.
- [51] Nawaz M, Hayat T, Alsaedi A. Mixed convection three-dimensional flow in the presence of hall and ion-slip effects. *J Heat Transf* 2013;135(4):042502.
- [52] Takhar HS, Chamkha AJ, Nath G. MHD flow over a moving plate in a rotating fluid with magnetic field, Hall currents and free stream velocity. *Int J Eng Sci* 2002;40 (13):1511–27.
- [53] Krishna MV, Ahamad NA, Chamkha AJ. Hall and ion slip effects on unsteady MHD free convective rotating flow through a saturated porous medium over an exponential accelerated plate. *Alexandria Eng J* 2020;59(2):565–77.
- [54] Nazir U, Mukdasai K. Combine influence of Hall effects and viscous dissipation on the motion of ethylene glycol conveying alumina, silica and titania nanoparticles using the non-Newtonian Casson model. *AIMS Math* 2023;8(2):4682–99.
- [55] Elsaid EM, AlShurafat KS. Impact of Hall current and Joule heating on a rotating hybrid nanofluid over a stretched plate with nonlinear thermal radiation. *J Nanofluids* 2023;12:548–56.
- [56] Bird RB, Stewart WE, Lightfoot EN. *Transport Phenomena*. New York: Wiley; 1960.
- [57] Lin YH, Zheng LC, Chen G. Unsteady flow and heat transfer of pseudo-plastic nanofluid in a finite thin film on a stretching surface with variable thermal conductivity and viscous dissipation. *Powder Technol* 2015;274:324–32.
- [58] Zheng LC, Lin YH, Zhang XX. Marangoni convection of power law fluids driven by power-law temperature gradient. *J Franklin Inst* 2012;349:2585–97.
- [59] Yan Z, Min Z, Bai Yu. Unsteady flow and heat transfer of power-law nanofluid thin film over a stretching sheet with variable magnetic field and power-law velocity slip effect. *J Taiwan Inst Chem Eng* 2017;70:104–10.
- [60] Bachok N, Ishak A, Pop I. Flow and heat transfer characteristics on a moving plate in a nanofluid. *Int J Heat and Mass Transfer* 2012;55:642–8.
- [61] Si X, Li H, Zheng L, Shen Y, Zhang X. A mixed convection flow and heat transfer of pseudo-plastic power law nanofluids past a stretching vertical plate. *Int J Heat and Mass Transfer* 2017;105:350–8.



Dr. M.K. Nayak is currently working as Associate Professor in the Department of Mechanical Engineering, Siksha 'O' Anusandhan Deemed to be University, Odisha, India. His research area includes Fluid Dynamics, Heat Transfer, Solar Thermal, Energy and Environment. His name has been appeared in the list of World's Top 2% of Scientists awarded by Stanford University, USA in the years 2020,2021,2022 and 2023. He has published 150 research articles to his credit. He has guided 5 Ph.D students and 10 M.Sc students in the areas of Fluid Dynamics, Heat Transfer and Energy.